

Chapter 2

Lower-crustal strength under the Dead Sea basin from local earthquake data and rheological modeling

F. Aldersons, Z. Ben-Avraham, A. Hofstetter, E. Kissling and T. Al-Yazjeen

Earth and Planetary Science Letters (2003) 214 129-142

ABSTRACT

We studied the local seismicity of the Dead Sea basin for the period 1984-1997. Sixty percent of well-constrained microearthquakes ($M_L \leq 3.2$) nucleated at depths of 20-32 km and more than 40 percent occurred below the depth of peak seismicity situated at 20 km. With the Moho at 32 km, the upper mantle appeared to be aseismic during the 14-year data period. A relocation procedure involving the simultaneous use of three regional velocity models reveals that the distribution of focal depths in the Dead Sea basin is stable. Lower-crustal seismicity is not an artifact created by strong lateral velocity variations or data-related problems. An upper bound depth uncertainty of ± 5 km is estimated below 20 km, but for most earthquakes depth mislocations should not exceed ± 2 km. A lithospheric strength profile has been calculated. Based on a surface heat flow of 40 mWm^{-2} and a quartz-depleted lower crust, a narrow brittle to ductile transition might occur in the crust around 380°C at a depth of 31 km. For the upper mantle, the brittle to ductile transition occurs in the model at 490°C and at 44 km depth. The absence of micro-seismicity in the upper mantle remains difficult to explain.

2.1 INTRODUCTION

It is commonly assumed (Meissner and Strehlau, 1982; Chen and Molnar, 1983) that no significant seismicity exists in rifts at depths greater than 15-20 km. The lower crust in continental extension zones is indeed often aseismic due to elevated temperatures accompanying lithospheric thinning. In relation to a more recent trend of research (Cloetingh and Burov, 1996; Maggi et al., 2000; Jackson, 2002), microearthquakes from Israel and Jordan suggest that the

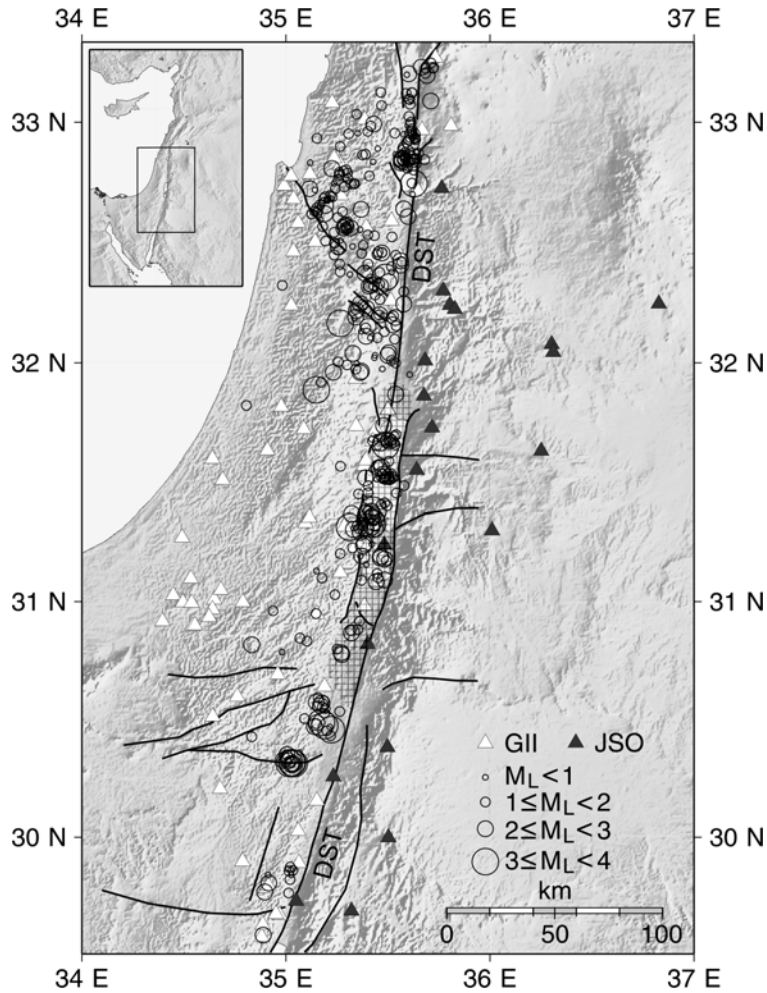


Figure 2.1 The Dead Sea region. Topographic shaded relief derived from Globe 1-km elevation data. The square grid fill defines the Dead Sea basin. Seismicity: 410 well-constrained earthquakes (1984-1997) recorded by short-period stations (triangles) of GII (Israel) and JSO (Jordan). DST: Dead Sea Transform.

lower crust (20-32 km) has probably kept a significant strength under the Dead Sea basin. A similar behavior of the lower crust in continental extension regimes has already been observed, mainly in the western branch of the East African rift system (Shudofsky et al., 1987; Nyblade and Langston, 1995; Camelbeek and Iranga, 1996) and in the Baikal rift system (Déverchère et al., 2001). Anomalous deep crustal earthquakes are also known to occur in the western United States (Wong and Chapman, 1990; Bryant and Jones, 1992) and below the northern Alpine foreland of Switzerland (Deichmann and Rybach, 1989). Focal depths of earthquakes are generally difficult to constrain tightly. The most reliable estimates are usually those derived from local earthquake data if well-distributed stations are present and a good knowledge of the velocity field has been gained. The Dead Sea basin and its surroundings (Figure 2.1) have been monitored locally for more than 10 years by permanent digital seismic stations. In addition, the

region has been the focus of detailed geophysical studies during past decades. These studies include bathymetry (Neev and Hall, 1979), seismic reflection (Neev and Hall, 1979; ten Brink and Ben-Avraham, 1989), seismic refraction (Ginzburg et al., 1981; Ginzburg and Ben-Avraham, 1997), gravity (ten Brink et al., 1990; ten Brink et al., 1993), magnetism (Frieslander and Ben-Avraham, 1989; Al-Zoubi and Ben-Avraham, 2002), heat flow (Ben-Avraham et al., 1978) and seismicity (van Eck and Hofstetter, 1989, 1990).

Constraints provided by these studies not only lead to more robust results, they also allow the development of geophysical models better tuned to the geological environment. In this article we present evidence from local earthquake data and rheological modeling that lead us to acknowledge the existence of a significant lower-crustal strength under the Dead Sea basin.

2.2 GEOLOGICAL SETTING

The Dead Sea Transform (Figure 2.1) is an intracontinental plate boundary resulting from the late-Cenozoic breakup of the Arabo-African continent. This boundary extends over 1,000 km from the zone of sea floor spreading at the southern tip of the Sinai Peninsula to the Taurus-Zagros zone of convergence in Turkey (Freund, 1965). The Dead Sea basin is an active pull-apart (Quennell, 1958) located along the Dead Sea Transform. The amount of left-lateral motion along the Transform in the Dead Sea region is estimated at 105 km (Quennell, 1958; Freund et al., 1970). Motion along the Transform started around 20 Ma ago during Miocene times (Bartov et al., 1980). Although the Dead Sea basin originated at the beginning of the Transform motion, it did not develop into a topographic low before early Pliocene (Garfunkel, 1997). Pliocene sediments are mostly composed of evaporites, among which halite is the main constituent. Deformation of Pliocene salt has created numerous diapirs in the basin (Neev and Hall, 1979). During Pleistocene times, basin subsidence accelerated (ten Brink and Ben-Avraham, 1989) and allowed the accumulation of several kilometers of lacustrine clastics, carbonates and evaporites. Today the basin is a morphotectonic depression over 130 km long and 7-18 km wide (Figure 2.1). It is a seismically active section (van Eck and Hofstetter, 1989, 1990) along the Dead Sea Transform, for which some 4,000 years of combined archaeological, historical and instrumental seismicities are documented (Ben-Menahem, 1991). For the northern half of the Dead Sea basin (main lake and salt pans), earthquakes of $M_L \geq 5.8 \pm 0.2$ have a recurrence interval of approximately 160 years (Shapira, 1997). The last earthquake of such a magnitude (estimated magnitude 6.2 by Turcotte and Arieh, 1988) occurred in the main lake (Shapira et al., 1993) in 1927 at an unknown depth.

2.3 SEISMICITY

Figure 2.2 displays a depth section of seismicity along the Dead Sea Transform between Aqaba-Elat in the south and the Sea of Galilee in the north for the period 1984-1997. Out of 2,283 routinely recorded events, a first selection resulted in 653 events with at least 8 P readings each and an azimuthal gap smaller than 180 degrees. To further exclude events with poorly constrained depths, an empirical criterion based on the epicentral distance to the nearest station (D_{min}) was adopted for events with an estimated depth of less than 21 km (Figure 2.3). For depths greater than 21 km, all events from the first selection appeared as valid candidates and were included. Two hundred forty-three events from the first selection of 653 events were rejected while the remaining were included and are the 410 earthquakes displayed in Figure 2.1 and Figure 2.2. Our study focuses on the Dead Sea basin and discusses whether the apparently unusual focal depths observed there are part of a broader phenomenon or represent a local anomaly.

We started the Dead Sea seismicity study by a series of relocations aimed at detecting flaws like unstable local minima solutions. Most first P arrivals from earthquakes nucleating in the basin were carefully repicked manually, and weighted according to the quality of their onsets. Forty-two well-constrained earthquakes qualified (Figure 2.4a) and relocations were performed with program Velest (Kissling, 1994).

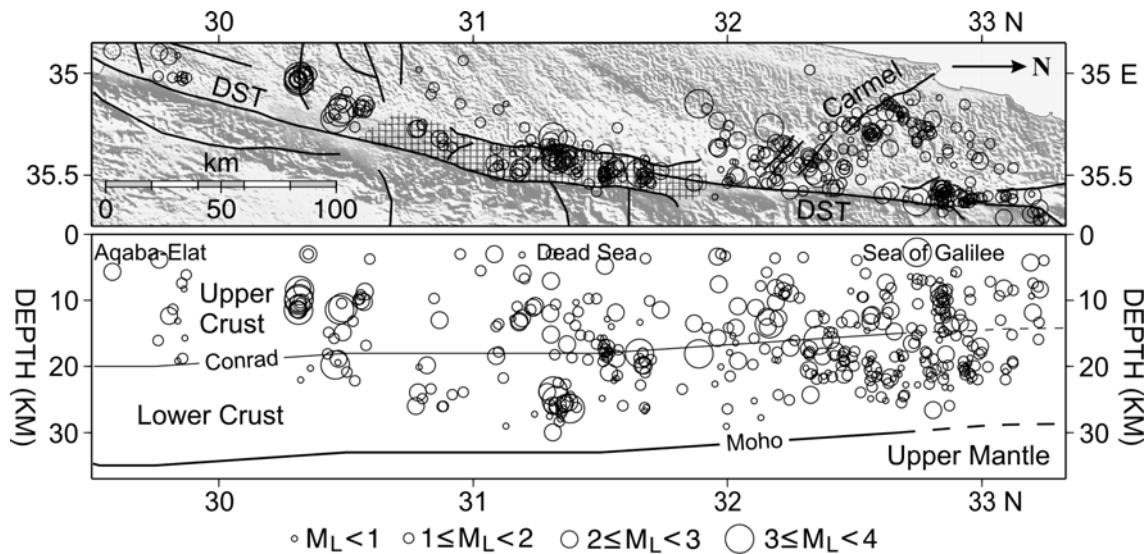


Figure 2.2 Depth section of well-constrained seismicity (410 earthquakes, 1984-1997) along the Dead Sea Transform (DST) from Aqaba-Elat to the Sea of Galilee. The square grid fill defines the Dead Sea basin on the map. Conrad and Moho discontinuities from Ginzburg et al. (1981).

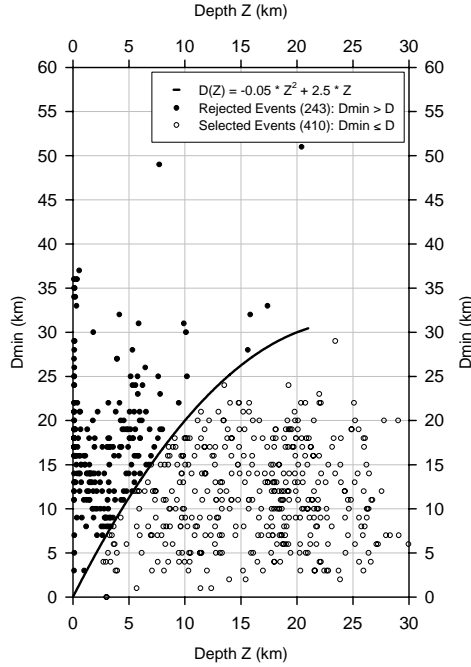


Figure 2.3 Near-epicentral distance selection for 653 events from Aqaba-Elat to the Sea of Galilee ($P \geq 8$ and Gap $< 180^\circ$). Z is the estimated hypocentral depth and D_{min} is the epicentral distance to the nearest station.

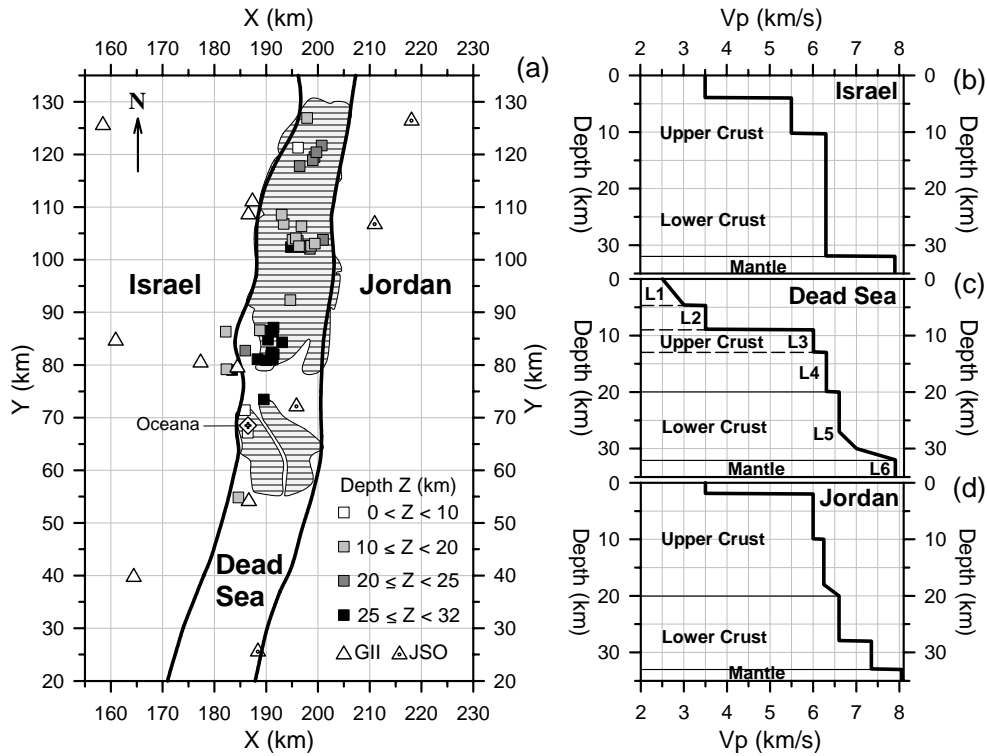


Figure 2.4 (a) Structural units and stations (triangles) in the Simulps relocation. Epicenters and depths of the set of 42 earthquakes (squares) relocated with Veltest. (X, Y) are Rectangular Israel Grid coordinates (Survey of Israel). Oceana is a salt quarry. (b,c,d) The three velocity models used in the Simulps relocation.

Model Israel (Figure 2.4b) was applied to the whole volume of earthquakes and stations. This model is similar to the routine model used by the Geophysical Institute of Israel (GII) but we derived it from quarry blasts located in the vicinity of the Dead Sea basin. Several relocations were conducted with Velest during which the effects of various initial conditions were explored. During these relocations, it was not considered a significant problem if the focal depths of a few earthquakes shifted up or down. Our main criterion was the stability of the distribution itself, not the perfect stability of every estimate. Tests like these are usually good at detecting flaws in hypocentral parameters like local minima solutions. No such flaws were ever observed. Depths derived from model Israel are stable. The distribution of depths in the Dead Sea basin is plotted in Figure 2.5a. It shows that 60 percent of well-constrained microearthquakes ($M_L \leq 3.2$) nucleated at depths of 20-32 km and that more than 40 percent occurred below the depth of peak seismicity situated at 20 km. The upper mantle appeared to be aseismic during the 14-year data period.

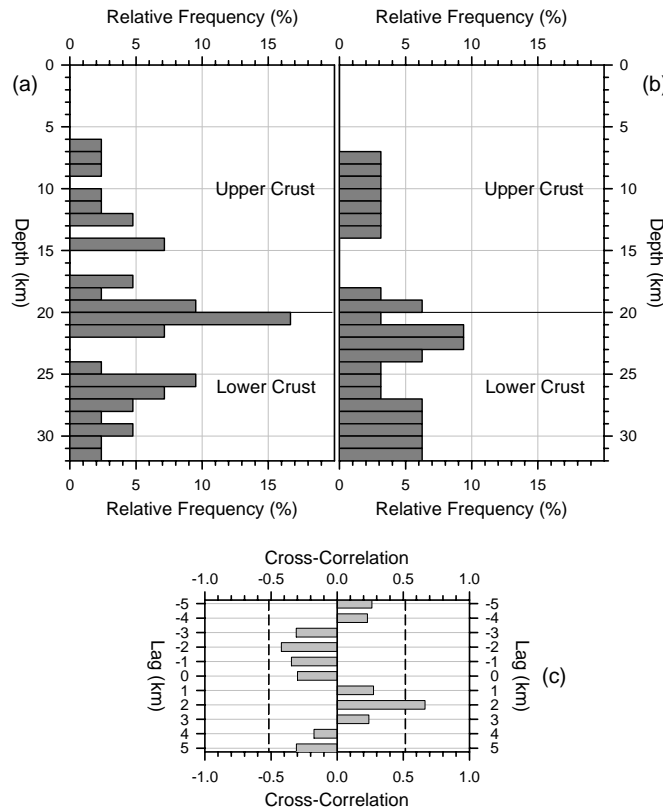


Figure 2.5 Focal depths of well-constrained earthquakes in the Dead Sea basin. (a) Depth distribution of 42 earthquakes located with regional velocity model Israel (Figure 2.4b) in Velest. (b) Depth distribution of 32 earthquakes located with three regional velocity models in Simulps (Figure 2.4). (c) Cross-correlation of (a) and (b) between 17 and 32 km depth. The dashed lines delineate the 95 % confidence interval assuming (a) and (b) to be uncorrelated. A significant correlation of 0.66 is found at Lag = + 2 km.

Although depths derived from model Israel are stable, velocities in the uppermost 9 km of the model are too high for the Dead Sea basin (compare model Israel versus model Dead Sea, Figure 2.4b and Figure 2.4c). This might create an artificial deepening of focal depths for earthquakes nucleating in the basin. In order to evaluate this possibility, program Simulps (Thurber, 1984) was also used to relocate earthquakes.

In each of the three structural units of Figure 2.4a, a one-dimensional velocity model was defined. The boundaries between the three units were derived from the maximum gradient of gravity (ten Brink et al., 1993). All three models are rather similar below the depth of 10 km. Models Israel and Jordan (El-Isa, 1990; JSO, 1993) are rather similar throughout. The first layer is however thinner in model Jordan compared to model Israel and no contrast between the upper and lower crust is present in model Israel. The upper crust in the Dead Sea velocity model was derived from a refraction profile in the north basin of the Dead Sea (Ginzburg and Ben-Avraham, 1997), while the lower crust was derived from a deep refraction experiment by Ginzburg et al. (1981). From the abrupt termination of the cusp (Bullen, 1960; Ginzburg et al., 1979), the authors infer the existence of a 5-km transition zone between the main lower-crustal velocity of 6.6 km/s and the upper mantle velocity of 7.9 km/s, a feature apparently missing in adjacent areas outside the rift. According to the same study, the Dead Sea basin is underlain by a Moho at about 32 km depth, a value supported by gravity modeling (ten Brink et al., 1993).

Earthquakes were relocated by Simulps according to the velocities and boundaries of the three structural units. No attempt was made to derive optimal velocities from the data themselves. The selection of a fine discretization grid resulted in restrictions on the maximum size of the model. Due to the smaller number of stations available, only 6 P arrivals were required for qualifying events. Among the 42 earthquakes relocated by Velest, 32 qualified for the Simulps relocation. Epicentral distances to stations never exceeded 85 kilometers and no more than 11 arrivals per earthquake could be observed. Most seismic rays were confined to the upper crust and rays from deeper earthquakes quickly turned up. Figure 2.5b displays the depth distribution using Simulps. The lower-crustal seismicity remains in place and the whole distribution displays features similar to those in the distribution computed with Velest, although deeper by 2 km in the lower half. Nearly identical results were obtained without the transition zone at the base of the lower crust. One should not however conclude that the Simulps relocation is more reliable than the Velest relocation. The purpose of the Simulps relocation was to test the possible influence of slow velocities in the upper section of the Dead Sea basin. The results show that the lower-crustal seismicity detected by Velest is not an artifact created by these slow basinal velocities.

Two independent evaluations of the uncertainty on depths derived from model Israel have been made. First, we applied perturbations to model Israel and relocated the 42 well-constrained earthquakes with resulting models in Velest. This method evaluates the sensitivity of depths to departures from model Israel, and it provides individual error bars for each of the 42 earthquakes. Velocity perturbations of $\pm 5\%$, $\pm 10\%$, and depth perturbations of $\pm 10\%$, $\pm 20\%$, were added to model Israel (Table 2.1 and Figure 2.6a). Velocity perturbations of $+10\%$ for layer 2 and -10% for layer 3 were not applied because they would have created some unrealistic velocity inversions with depth from layer 2 to layer 3. Consequently and in order to preserve symmetry around model Israel, velocity perturbations of -10% for layer 2 and $+10\%$ for layer 3 were also not applied. The bottom depth of layer 3 (the Moho) was not perturbed by more than $\pm 9\%$ following gravity results implying that the Moho should not be anomalously elevated by more than 2-3 km under the Dead Sea basin (ten Brink et al., 1990; ten Brink et al., 1993). Perturbations of ± 0.250 km/s around the upper mantle velocity of 7.9 km/s appeared also to be quite sufficient. All combinations of perturbations defined in Table 2.1 represent a set of 16,875 velocity models.

Depths and error bars derived from this set are plotted in Figure 2.6b. Two main conclusions emerge. First, according to the 5th to 95th percentile intervals, at least 25 % of well-constrained microearthquakes under the Dead Sea basin can belong neither to the upper-crustal seismicity nor to a hypothetical upper-mantle seismicity. Second, error bars tend to narrow for deeper earthquakes (Figure 2.7), expressing a lesser sensitivity to model perturbations in the lower crust compared to the upper crust.

Table 2.1 Perturbations to model Israel

Layer	V_p (km/s)	V_p perturbation (%)	Layer bottom (km)	Bottom perturbation (%)
Layer 1	3.150	-10.0 %	3.280	-20.0 %
	3.325	-5.0 %	3.690	-10.0 %
	3.500	0.0 %	4.100	0.0 %
	3.675	+5.0 %	4.510	+10.0 %
	3.850	+10.0 %	4.920	+20.0 %
Layer 2			8.640	-20.0 %
	5.225	-5.0 %	9.720	-10.0 %
	5.500	0.0 %	10.800	0.0 %
	5.775	+5.0 %	11.880	+10.0 %
			12.960	+20.0 %
Layer 3			29.000	-9.1 %
	5.985	-5.0 %	30.450	-4.5 %
	6.300	0.0 %	31.900	0.0 %
	6.615	+5.0 %	33.350	+4.5 %
			34.800	+9.1 %
Layer 4	7.650	-3.2 %	Half-space	
	7.900	0.0 %		
	8.150	+3.2 %		

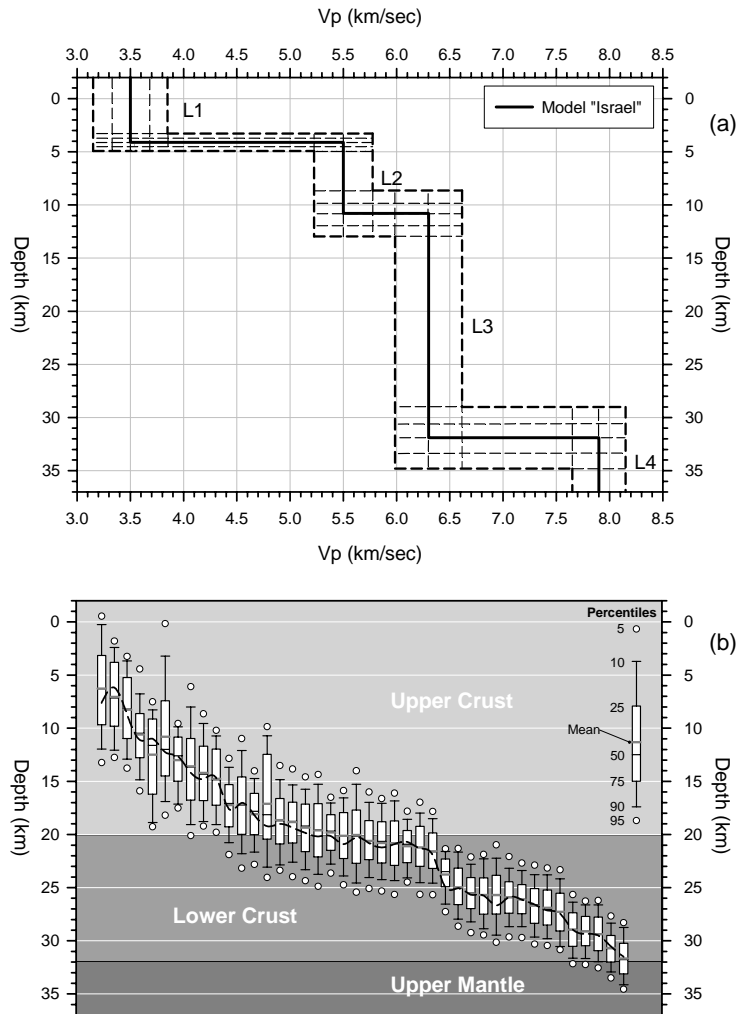


Figure 2.6 (a) Depth and velocity perturbations defining 16,875 models around model Israel. L1 to L4 are the four layers of model Israel. (b) Hypocentral depths and error bars for the 42 earthquakes relocated by Velest with perturbed models defined in (a). Earthquakes sorted according to increasing median (50th percentile) depth. The black dashed line marks depths obtained with model Israel.

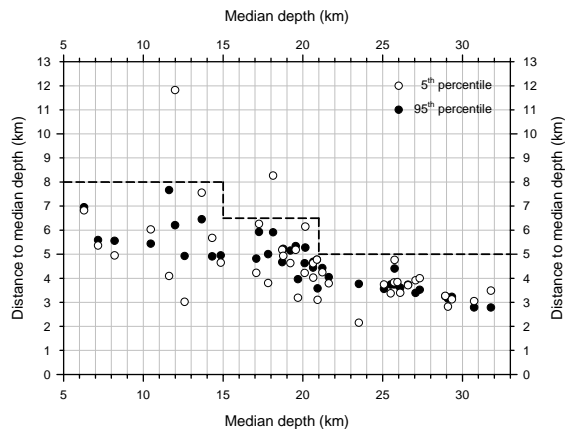


Figure 2.7 Upper-bound to the uncertainty on depths (dashed line) from perturbations to model Israel.

This is a coherent behavior of a distribution of depths since seismic rays from shallower earthquakes tend to propagate twice (by refraction) through more layers than deeper earthquakes do. Error bars show also that several lower-crustal earthquakes close to 20 km depth could have nucleated in the upper crust but the reverse is also true, a similar number of upper-crustal earthquakes could have nucleated in the lower crust. The net result is then very close to the original distribution of depths. Close to the Moho, only the two deepest earthquakes are realistic candidates for an upper-mantle origin but model Israel locates them in the lower crust. From Figure 2.7, an upper-bound to the uncertainty in the range of depths 21-32 km is then ± 5 km.

As a second approach to depth uncertainties, we determined true depth errors for a series of blasts from quarry Oceana. Oceana is a Dead Sea salt quarry located on the western salt pan south of the main lake and only 15 km away from the main cluster of deepest earthquakes (Figure 2.4a). We only considered well-constrained blasts with at least 8 P readings, and an azimuthal gap not greater than 150 degrees. In addition, we required Dmin (distance of closest station to the estimated epicenter) to be 3-4 km and we rejected events not explicitly attributed to Oceana by the GII analysts. Figure 2.8 shows that the number of P readings for the 24 Oceana blasts is lower than for the 42 earthquakes while gaps are similar. It shows also that earthquakes below 20 km depth have all a Dmin value lower than the estimated depth, an important feature regarding depth control. As a whole, Oceana blast data are then not as well-constrained as our set of earthquakes.

Nevertheless, Figure 2.9b reveals that Oceana blasts located with model Israel do not display true depth errors greater than 2 km, with the exception of two outliers. Since blast locations are generally less accurate than earthquake locations in a given area due to poorly approximated refracted rays near sources at the surface (Kissling, 1988), even smaller depth mislocations are possible for earthquakes in the basin.

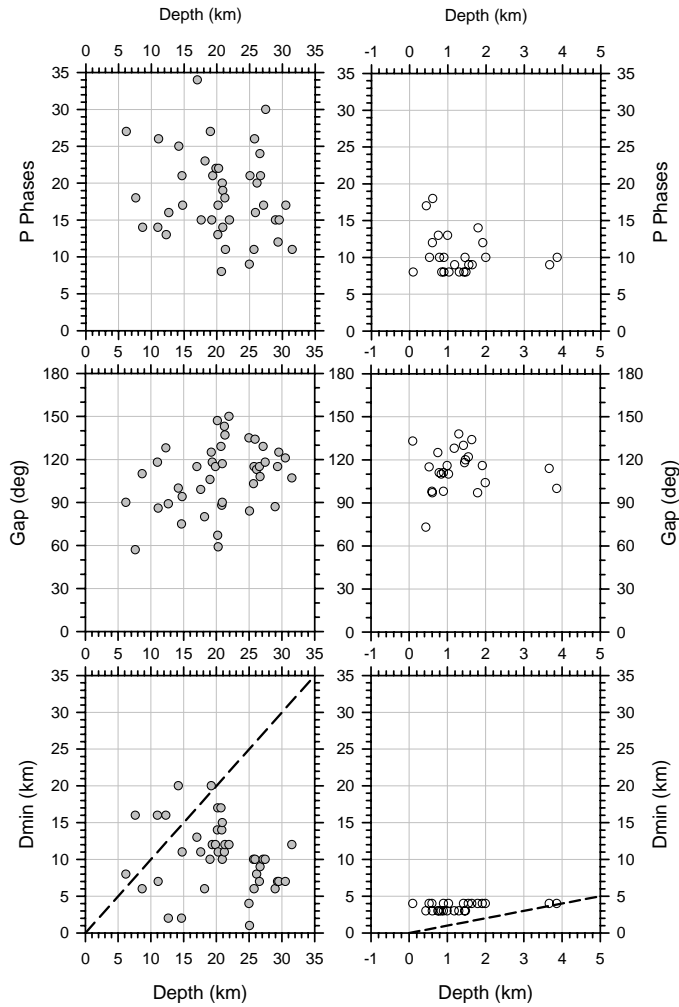
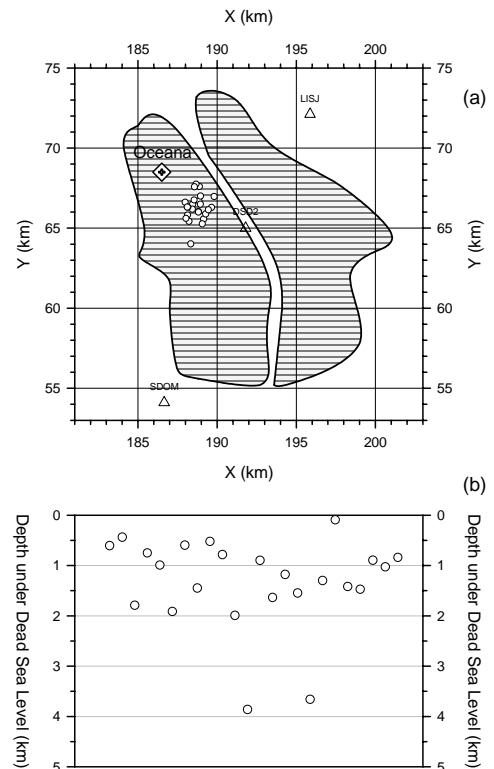


Figure 2.8 (Left) Number of P phases, azimuthal gap and Dmin for the 42 earthquakes located with model Israel in Velest. (Right) Same as (Left) but for 24 blasts of quarry Oceana. Dmin is the distance of the closest station to the estimated epicenter. The dashed line outlines values for which Dmin is equal to the estimated depth.

Figure 2.9 (a) Epicentral locations (model Israel in Velest) of 24 Oceana quarry blasts. X and Y are Cassini-Soldner (Survey of Israel) projection coordinates. Epicenters as white circles. (b) Depth error of blasts plotted in (a).



2.4 RHEOLOGY

A lithospheric strength profile (e.g. Ranalli, 1987) has been calculated using the five crustal layers defined in velocity model Dead Sea (Figure 2.4c) and one additional layer for the upper mantle. Below 20 km, the lower crust was modeled as diabase, a lithology consistent with the main value of 6.6 km/s (Christensen and Mooney, 1995) in layer 5 of the velocity model. The transition zone at the base of the crust was discarded.

We derived the geotherm for the Dead Sea basin from the one-dimensional equilibrium heat conduction (Turcotte and Schubert, 2002) equation

$$\frac{\partial^2 T}{\partial z^2} = -\frac{A}{k} \quad (2.1)$$

where T is the temperature, z the depth, A the radiogenic heat generation rate per unit volume, and k the thermal conductivity. This second-order differential equation can be solved given two boundary conditions. Assuming the surface to be at $z = 0$ and z increasing with depth, the surface heat flow and surface temperature as boundary conditions are respectively $Q = -k\partial T / \partial z = -Q_0$ at $z = 0$, and $T = T_0$ at $z = 0$. The surface heat flow $Q = -Q_0$ is negative because heat is flowing upwards and z is positive downwards. For a layered model where each layer i has a given thermal conductivity k_i and a radiogenic heat generation rate A_i , we obtain the temperature $T_{n,z}$ in layer n at a depth z from the surface:

$$T_{n,z} = -\frac{A_n}{2k_n} z^2 + \left[\sum_{i=1}^{n-1} \left(\frac{A_{i+1}}{k_{i+1}} - \frac{A_i}{k_i} \right) z_i + \frac{Q_0}{k_1} \right] z + \sum_{i=1}^{n-1} \left(\frac{A_i}{2k_i} - \frac{A_{i+1}}{2k_{i+1}} \right) z_i^2 + T_0 \quad (2.2)$$

where z_i is the bottom depth of layer i . Using six layers and average parameters, the one-dimensional geotherm is only sensitive to two variables: the surface heat flow, and the thermal conductivity in the first layer. These two variables exert a great influence on the slope of the geotherm at the surface and therefore play a major role on the estimated temperature in the deeper part of the model. The average measured heat flow in the northern Dead Sea basin is 38 mWm⁻² (Ben-Avraham et al., 1978; Ben-Avraham, 1997) and it is 42 mWm⁻² (Eckstein and Simmons, 1978) west of the basin. These values are very similar to the uniform heat flow measured in the eastern Mediterranean (Erickson, 1970). Consequently, the surface heat flow Q_0 of 40 ± 2 mWm⁻² we used to compute the equilibrium geotherm appears to be well constrained. The surface temperature T_0 was set in the model at 5 °C. Regarding the first layer, Plio-Pleistocene to recent sediments are composed of fluvial and lacustrine clastics, marls, chalks and evaporites. The few quaternary conductivities available in the Dead Sea basin (Eckstein and Simmons, 1978) are very low (1.25 Wm⁻¹K⁻¹) but were measured through only the first 150 m

from the surface. In order to get a brittle to ductile transition around 30 km with a surface heat flow of 40 mWm^{-2} , a mean thermal conductivity of at least $2.1 \text{ Wm}^{-1}\text{K}^{-1}$ is required in the first layer. This figure appears as a realistic value taking into account compaction and a content of 5-10 percent of highly conductive evaporites in the first layer. It is unlikely that the true value over the thickness (4.7 km) of the first layer would be lower than $2.0 \text{ Wm}^{-1}\text{K}^{-1}$.

The radiogenic heat generation rate is poorly constrained in the Dead Sea region. However, about 110 m of recent sediments from two cores (Stiller et al., 1985) taken in the Dead Sea lake contained on the average 3.87 ppm of ^{238}U , 4.15 ppm of ^{232}Th and 1.1 ppm of ^{40}K . These U and Th values are within the normal range of sedimentary materials found worldwide (Rodgers and Adams, 1969). For layers 1 and 2 of density $2,150 \text{ kgm}^{-3}$ and $2,550 \text{ kgm}^{-3}$, the total heat generation rate A is then (Beardsmore and Cull, 2001) 1.0 and $1.2 \text{ }\mu\text{Wm}^{-3}$ respectively. For the crustal plutonic rocks of the model, we used the relations between the velocity of P waves V_p and the heat generation rate A of Rybach and Buntebarth (1984). With their relation for Phanerozoic rocks, we obtained (at 200 MPa) 2.27 and $1.27 \text{ }\mu\text{Wm}^{-3}$ for layer 3 (granite) and layer 4 (quartz diorite) respectively. To account for the fact that the last stage of major regional plutonism occurred (Garfunkel, 1999) during late Proterozoic (Pan-African orogeny), we applied an arbitrary correction of -20 % to the computed values. The adopted heat generation rates for layers 3 and 4 are then 1.8 and $1.0 \text{ }\mu\text{Wm}^{-3}$ respectively. For layer 5 (diabase), the Rybach-Buntebarth relation for Precambrian rocks led to a value of $0.2 \text{ }\mu\text{Wm}^{-3}$. An average value of $0.007 \text{ }\mu\text{Wm}^{-3}$ (Ranalli, 1987) was adopted for the upper mantle.

A frictional (brittle) failure criterion following Byerlee's law of friction (Byerlee, 1968, 1978) can be expressed from Anderson's theory of faulting (Anderson, 1951) as (Sibson, 1974; Ranalli, 1987)

$$\sigma_1 - \sigma_3 = \alpha \rho g z (1 - \lambda) \quad (2.3)$$

where $\sigma_1 - \sigma_3$ is the failure stress, α a parameter depending on the type of faulting, ρ the average density, g the acceleration of gravity, z the depth, and λ is the ratio of pore fluid pressure to lithostatic pressure. For a friction coefficient of 0.75, values of the fault parameter α are 3.0, 1.2 and 0.75 for thrust, strike-slip and normal faults respectively (Sibson, 1974; Ranalli, 1987). We adopted an intermediate value α of 1.05 between strike-slip and normal faulting as earthquake focal mechanisms (van Eck and Hofstetter, 1989) and seismic reflection profiles (ten Brink and Ben-Avraham, 1989) show that both types of faults coexist in the basin. The average density ρ in the model is $2,670 \text{ kgm}^{-3}$ for the crust, and $3,370 \text{ kgm}^{-3}$ (Turcotte and Schubert, 2002) for the upper mantle above the 220 km discontinuity. The pore fluid pressure was set at an intermediate

value between hydrostatic and dry. Equation 2.3 provides a lower limit to the failure stress because it assumes an ideal orientation of faulting with respect to the stress field.

Ductile deformation in the crust is dominated by power-law creep (dislocation climb) given (e.g. Ranalli, 1987) by

$$\sigma_1 - \sigma_3 = \left(\frac{\dot{\varepsilon}}{D} \right)^{\frac{1}{n}} e^{\frac{E_C}{nRT}} \quad (2.4)$$

where $\sigma_1 - \sigma_3$ is the flow stress for a given strain rate, $\dot{\varepsilon}$ the strain rate, D the Dorn parameter, n the stress exponent, E_C the creep activation energy, R the gas constant, and T is the temperature. Values for D , n and E_C are provided in Table 2.2.

Table 2.2 Dislocation climb (power-law) creep parameters

Rock / Mineral	Layer	D (Pa ⁻ⁿ s ⁻¹)	n	E_C (kJ mol ⁻¹)
Quartzite (wet) ¹	1, 2	3.99×10^{-18}	2.3	154
Granite ¹	3	7.92×10^{-29}	3.2	123
Quartz diorite ²	4	5.02×10^{-18}	2.4	219
Diabase ³	5	8.04×10^{-25}	3.4	260
Olivine ⁴	6	7.00×10^{-14}	3.0	511

D is the Dorn parameter, n the stress exponent and E_C is the creep activation energy.

¹ From Ranalli and Murphy (1987), data from compilation of Kirby (1983).

² From Kirby (1983), data from Hansen and Carter (1982).

³ From Kirby (1983), data from Shelton and Tullis (1981).

⁴ From Goetze (1978).

In the mantle, ductile deformation is controlled by the power-law creep (equation 2.4) of olivine only for deviatoric stresses below 200 MPa. For deviatoric stresses greater than 200 MPa, the glide-controlled creep of olivine is assumed to dominate (Goetze, 1978; Kameyama et al., 1999):

$$\sigma_1 - \sigma_3 = \sigma_0 \left(1 - \left[\frac{RT}{E_p} \ln \left(\frac{\dot{\varepsilon}_0}{\dot{\varepsilon}} \right) \right]^{\frac{1}{2}} \right) \quad (2.5)$$

In equation 2.5, σ_0 is the Peierls reference stress, E_p the activation energy for the Peierls mechanism, and $\dot{\varepsilon}_0$ is the reference strain rate. Values for σ_0 , E_p and $\dot{\varepsilon}_0$ are provided in Table 2.3.

Table 2.3 Dislocation glide creep parameters

Rock / Mineral	Layer	σ_0 (Pa)	$\dot{\epsilon}_0$ (s ⁻¹)	E_p (kJ mol ⁻¹)
Olivine	6	8.5×10^9	5.7×10^{11}	535

σ_0 is the Peierls reference stress, E_p the activation energy for the Peierls mechanism, and $\dot{\epsilon}_0$ is the reference strain rate. Data from Goetze (1978).

A strain rate $\dot{\epsilon}$ of $2 \times 10^{-15} \text{s}^{-1}$ was used in the model. This value was derived from a relative plate motion of 5 mm/yr, an intermediate value between short-term global positioning results of 2.6 ± 1.1 mm/yr (Pe'eri et al., 2002) and long-term geological estimates of 6-10 mm/yr (Quennell, 1958; Freund, 1965).

At a given depth, the smaller value of the failure stress and the flow stress gives the yield strength. A rheological profile (strength envelope) is a curve of yield strength versus depth. At low temperatures, the failure stress is lower than the flow stress and brittle behavior dominates the deformation of rocks. The opposite is true at high temperatures where aseismic ductile behavior prevails. The usually sharp brittle to ductile transitions in the lithosphere are supposed to correspond to boundaries of seismogenic zones. Several brittle to ductile transitions and related seismogenic zones can occur in the lithosphere. The interpretation of strength profiles is based on rather strong assumptions (Scholz, 2002) but the method provides a useful first-order estimate of the rheology.

Figure 2.10 displays the results with a surface heat flow of 40 mWm^{-2} and a thermal conductivity of $2.1 \text{ Wm}^{-1}\text{K}^{-1}$ in the first layer. A narrow brittle to ductile transition occurs in the crust around 380°C at 31 km depth. With a heat flow of 42 mWm^{-2} and a conductivity of $2.0 \text{ Wm}^{-1}\text{K}^{-1}$ in the first layer, the transition would occur around 390°C at a depth of 26 km. However, parameters we adopted from Shelton and Tullis (1981) for diabase in the lower crust do not represent dry deformation conditions, as their samples were only dried at 160°C . A recent experimental study on the creep of diabase (Mackwell et al., 1998) revealed that this type of rock is significantly stronger under truly dry conditions. Consequently, if the lower crust under the Dead Sea basin has a basaltic composition and is dry, it should even be ductilely stronger than what we report. In that case, no brittle to ductile transition would occur at all in the lower crust except for unrealistic Moho temperatures above 600°C and related surface heat flows greater than 55 mWm^{-2} . In the upper mantle, the brittle to ductile transition occurs in the model at 44 km depth and at 490°C but as said earlier, the upper mantle appears to be aseismic during the 14-year data period.

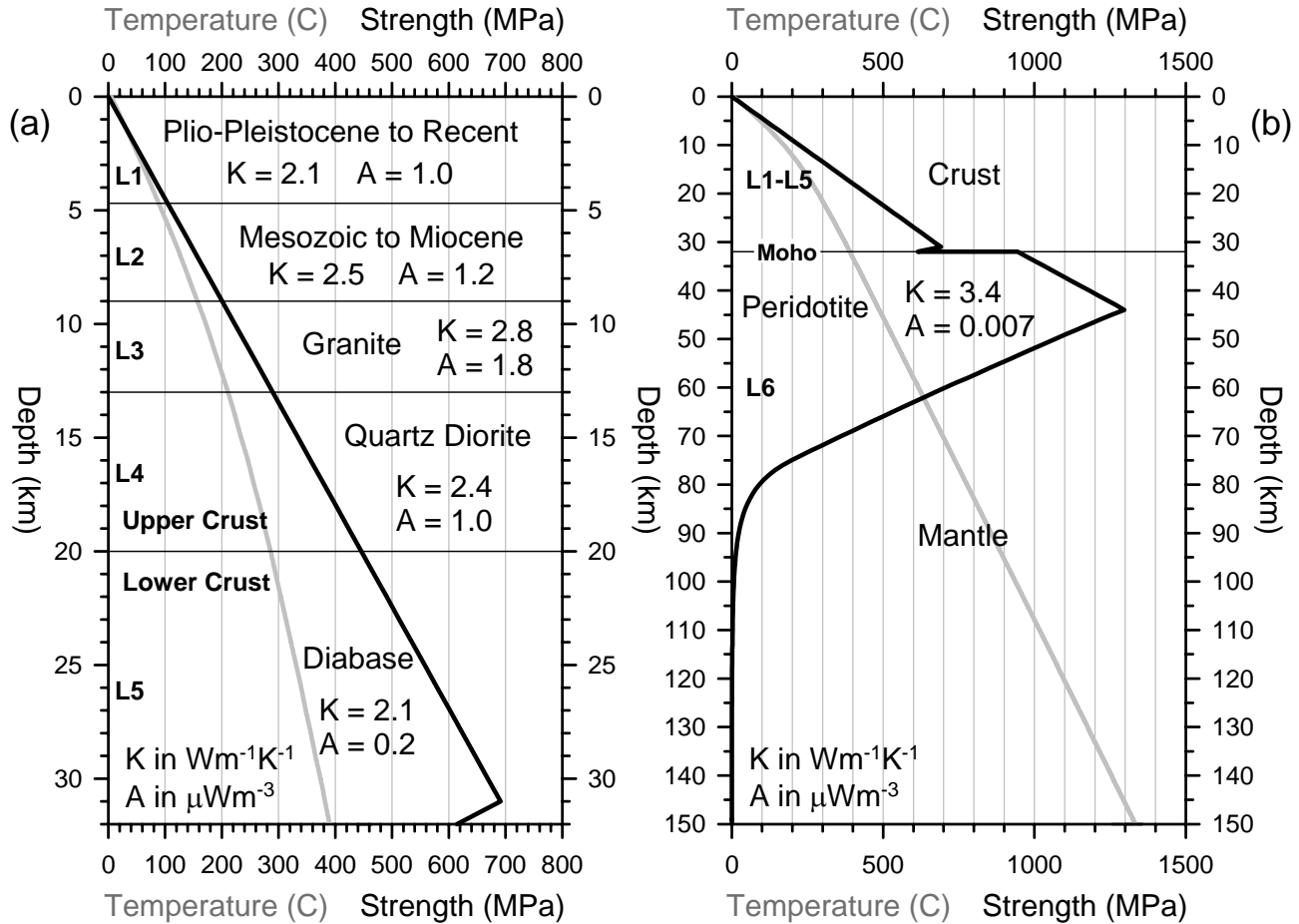


Figure 2.10 Rheology of the Dead Sea basin. (a) Crustal geotherm (gray) and strength profile (black). (b) Lithospheric geotherm (gray) and strength profile (black). Surface heat flow of 40 mWm^{-2} . K is the thermal conductivity and A is the radiogenic heat production rate.

2.5 DISCUSSION AND CONCLUSIONS

In the Dead Sea basin, well-constrained microearthquakes ($M_L \leq 3.2$) display continuous focal depths down to the Moho located at a depth of 32 km. Sixty percent of these well-constrained microearthquakes nucleated at depths of 20-32 km and more than 40 percent occurred below the depth of peak seismicity situated at 20 km. An upper bound uncertainty of ± 5 km is estimated for depths greater than 20 km, but depth mislocations should not exceed ± 2 km for most earthquakes. No data support the view that lower-crustal seismicity could be nothing more than an artifact due to earthquakes actually nucleating in the upper crust or in the upper mantle. Due to uncertainties on focal depths, a few earthquakes might well have nucleated in the upper mantle but a distinct population of upper mantle earthquakes is missing.

Most parameters in rheological modeling are commonly poorly constrained, and the method itself suffers from inherent limitations (Scholz, 2002). Therefore, strength envelopes generally cannot serve to accurately estimate the thickness of the seismogenic zone. In the case of the Dead Sea basin, we are merely able to say that a brittle to ductile transition around 31 km depth (where semi-brittle failure would prevail) is consistent with a surface heat flow of 40 mWm^{-2} . The low value of the regional surface heat flow is a good indication that the lower crust might be cool and brittle. Nevertheless, since conductive thermal anomalies can take millions of years to reach the surface, the surface heat flow does not always reflect lower-crustal temperatures. With such a clear lower-crustal seismicity as the one monitored in the Dead Sea basin, a significant departure from the equilibrium geotherm is however not expected. It appears therefore valid to use the equilibrium geotherm to extrapolate temperatures to lower-crustal depths. The estimated temperature of 380°C at the brittle to ductile transition is clearly below the temperature of 450°C ($350 \pm 100^\circ\text{C}$) generally considered (Chen and Molnar, 1983) as the limiting temperature of the deepest crustal seismogenic zone. In addition, a crustal seismic investigation of the Afro-Arabian rifts (Prodehl et al., 1997) shows that upper mantle Pn velocities close to 8.0 km/s as found under the Dead Sea (Ginzburg et al., 1981) are more typical of cooler rift flanks than of rifts axes, where slower velocities are usually observed due to anomalous heating. If brittle behavior is then likely to be the dominant deformation mechanism in the lower crust of the basin, strong earthquakes should also nucleate in the lower crust and not only microearthquakes as we report. Unfortunately, due to the long recurrence interval of strong earthquakes in the Dead Sea (Shapira, 1997), several centuries of monitoring might be required before valid statistics would allow a reliable assessment of this likely possibility. As an alternative solution to a brittle lower crust, a model recently developed by Al-Zoubi and ten Brink (2002; ten Brink, 2002) suggests that crustal flow might well be a viable deformation mechanism in the lower crust of the Dead Sea basin. Although this is not what our results mostly suggest, it remains a possibility with a higher heat flow and a lower crust made of wet diabase, or if quartz diorite substitutes for diabase. Around 400°C , a dry diabase would be ductilely too strong and brittle failure would prevail.

If the lower crust of the Dead Sea is cool and brittle, then the upper mantle should also be in a seismogenic state but appears to be aseismic during the 14-year data period. This apparent paradox is in agreement with Maggi et al. (2000), Jackson (2002) and earlier studies (Banda and Cloetingh, 1992; Cloetingh and Burov, 1996) regarding the general scarcity of events in the upper mantle of continents. Cloetingh and Burov (1996) suggest a few possible explanations: stress relaxation due to crust-mantle decoupling, strengthening of the uppermost mantle in downward-bent rift basins and low or inhomogeneous horizontal intraplate stress. Finally, the

mantle lithosphere may also not be so ductilely strong as suggested by laboratory experiments. This last explanation is adopted by Maggi et al. (2000) and Jackson (2002), following the observation (McKenzie and Fairhead, 1997; Maggi et al., 2000) that the effective elastic thickness T_e of the continental lithosphere is usually close to the thickness of the seismogenic crust T_s . Consequently, the mantle would have no significant strength. In the case of the Baikal rift, an effective elastic thickness T_e larger than the total crustal thickness leads Déverchère et al. (2001) to a different conclusion. The authors argue that on the contrary, the high strength of the mantle is the reason explaining the scarcity of earthquakes below the Moho. The upper mantle would not be aseismic but nucleation of earthquakes would be difficult, leading to long recurrence intervals. In the case of the Dead Sea basin, we do not see decoupling between the crust and the mantle as a likely mechanism explaining the absence of earthquakes in the upper mantle, our results pointing towards a mechanically coupled crust-mantle. Unfortunately, this is the only data-driven conclusion we can reach so far about this difficult and controversial subject.

Earthquakes between Aqaba-Elat and the Sea of Galilee were also relocated with the same requirements and velocity model used to derive the distribution of depths in the Dead Sea basin. According to the distribution of focal depths (Figure 2.2), the Dead Sea Transform is not accompanied by any crustal thermal anomaly between the Dead Sea basin and the Sea of Galilee. In this region, deep-crustal seismicity is not only observed along the Dead Sea Transform but also along the Carmel fault zone off the Transform. Southward, the deepest earthquakes quickly become shallower, and barely reach the lower crust in the region of Aqaba-Elat. With appropriate adjustments in rheological models, the maximum depth of approximately 20 km in this region is consistent with the surface heat flow of 65 mWm^{-2} measured in the northern part of the Gulf of Aqaba-Elat (Ben-Avraham and Von Herzen, 1987). The thinning of the seismogenic zone in the region of Aqaba-Elat is probably related more to the increase in the regional heat flow toward the Red Sea (Ben-Avraham and Von Herzen, 1987) than to a heat anomaly directly associated with the Dead Sea Transform itself.

ACKNOWLEDGMENTS

We thank S. Wdowinski for his help during the early stage of rheological modeling. We benefited from stimulating discussions with M. Steckler and S. Feinstein. We are also thankful to Uri ten Brink, Sierd Cloetingh, an anonymous reviewer, and the editor Scott King for their in-depth criticism and advice. F.A. was supported by a Ph.D. grant from the Ministry of Energy and Infrastructure of Israel.

REFERENCES

- Al-Zoubi, A., and Ben-Avraham, Z. (2002) Structure of the earth's crust in Jordan from potential field data. *Tectonophysics*, 346, 45-59.
- Al-Zoubi, A., and ten Brink, U. (2002) Lower crustal flow and the role of shear in basin subsidence: an example from the Dea Sea basin. *Earth and Planetary Science Letters*, 199, 67-79.
- Anderson, E.M. (1951) *The Dynamics of Faulting*, 2nd edition. Oliver and Boyd, Edinburgh, England.
- Banda, E., and Cloetingh, S. (1992) Physical properties of the Europe's lithosphere. In Blundell, D., Freeman, R., and Mueller, S. (Eds.) *A continent revealed: The European Geotraverse*: Cambridge University Press, Cambridge, 71-80.
- Bartov, Y., Steinitz, G., Eyal, M., and Eyal, Y. (1980) Sinistral movement along the Gulf of Aqaba – its age and relation to the opening of the Red Sea. *Nature*, 285, 220-221.
- Beardsmore, G.R., and Cull, J.P. (2001) *Crustal Heat Flow: a guide to measurement and modeling*. Cambridge University Press, Cambridge.
- Ben-Avraham, Z. (1997) Geophysical framework of the Dead Sea: structure and tectonics. In Niemi, T.M., Ben-Avraham, Z., and Gat, J.R. (Eds.) *The Dead Sea: The lake and its settings*: Oxford University Press, New York, NY, 36, 22-35.
- Ben-Avraham, Z., and Von Herzen, R.P. (1987) Heat flow and continental breakup: the Gulf of Elat (Aqaba). *Journal of Geophysical Research*, 92, 1407-1416.
- Ben-Avraham, Z., Hänel, R., and Villinger, H. (1978) Heat flow through the Dead Sea rift. *Marine Geology*, 28, 253-269.
- Ben-Menahem, A. (1991) Four Thousand Years of Seismicity Along the Dead Sea Rift. *Journal of Geophysical Research*, 96, B12, 20195-20216.
- Bryant, A.S., and Jones, L.M. (1992) Anomalously Deep Crustal Earthquakes in the Ventura Basin, Southern California. *Journal of Geophysical Research*, 97, 437-447.
- Bullen, K.E. (1960) Note on Cusps in Seismic Travel-Times. *Geophysical Journal of the Royal Astronomical Society*, 3, 354-359.
- Byerlee, J.D. (1968) Brittle-ductile transition in rocks. *Journal of Geophysical Research*, 73, 4741-4750.
- Byerlee, J.D. (1978) Friction of rocks. *Pure and Applied Geophysics*, 116, 615-626.
- Camelbeek, T., and Iranga, M.D. (1996) Deep crustal earthquakes and geometry of active faults along the Rukwa trough, East Africa. *Geophysical Journal International*, 124, 612–630.

- Chen, W-P., and Molnar, P. (1983) Focal depths of intracontinental and intraplate earthquakes and their implications for the thermal and mechanical properties of the lithosphere. *Journal of Geophysical Research*, 88, B5, 4183-4214.
- Christensen, N.I., and Mooney, W.D. (1995) Seismic velocity structure and composition of the continental crust: a global view. *Journal of Geophysical Research*, 100, B7, 9761-9788.
- Cloetingh, S., and Burov, E. (1996) Thermomechanical structure of European continental lithosphere: constraints from rheological profiles and EET estimates. *Geophysical Journal International*, 124, 695-723.
- Deichmann, N., and Rybach, L. (1989) Earthquakes and temperatures in the lower crust below the northern alpine foreland of Switzerland. In Mereu, R.F., Mueller, S., Fountain, D.M., (Eds.) *Properties and processes of the Earth's Lower Crust: Geophysical Monograph 51*, IUGG, Vol. 6, American Geophysical Union, Washington, DC, 197-213.
- Déverchère, J., Petit, C., Gileva, N., Radziminovitch, N., Melnikova, V., and San'kov, V. (2001) Depth distribution of earthquakes in the Baikal rift system and its implications for the rheology of the lithosphere. *Geophysical Journal International*, 146, 714-730.
- Eckstein, Y., and Simmons, G. (1978) Measurements and interpretation of terrestrial heat flow in Israel. *Geothermics*, 6, 117-142.
- El-Isa, Z.H. (1990) Lithospheric structure of the Jordan-Dead Sea transform from earthquake data. *Tectonophysics*, 180, 29-36.
- Erickson, A.J. (1970) The measurement and interpretation of heat flow in the Mediterranean and Black Sea. Ph.D. thesis, Massachusetts Institute of Technology, pp. 433.
- Freund, R. (1965) A model of the structural development of Israel and adjacent areas since Upper Cretaceous times. *Geological Magazine*, 102, 189-205.
- Freund, R., Garfunkel, Z., Zak, I., Goldberg, M., Weissbrod, T., and Derin, B. (1970) The shear along the Dead Sea rift. *Philosophical Transactions of the Royal Society of London, Series A*, 267, 105-127.
- Frieslander, U., and Ben-Avraham, Z. (1989) Magnetic field over the Dead Sea and vicinity. *Marine and Petroleum Geology*, 6, 148-160.
- Garfunkel, Z. (1997) The history and formation of the Dead Sea basin. In Niemi, T.M., Ben-Avraham, Z., and Gat, J.R. (Eds.) *The Dead Sea: The lake and its settings: Oxford University Press*, New York, NY, 36, 36-52.
- Garfunkel, Z. (1999) History and paleogeography during the Pan-African orogen to stable platform transition: Reappraisal of the evidence from the Elat area and the northern Arabian-Nubian Shield. *Israel Journal of Earth Sciences*, 48, 135-157.
- Ginzburg, A., and Ben-Avraham, Z. (1997) A seismic refraction study of the north basin of the Dead Sea, Israel. *Geophysical Research Letters*, 24, 2063-2066.

- Ginzburg, A., Makris, J., Fuchs, K., and Prodehl, C. (1981) The structure of the crust and upper mantle in the Dead Sea rift. *Tectonophysics*, 80, 109-119.
- Ginzburg, A., Makris, J., Fuchs, K., Perathoner, B., and Prodehl, C. (1979) Detailed Structure of the Crust and Upper Mantle Along the Jordan-Dead Sea Rift. *Journal of Geophysical Research*, 84, B10, 5605-5612.
- Goetze, C. (1978) The mechanisms of creep in olivine. *Philosophical Transactions of the Royal Society of London, Series A*, 288, 99-119.
- Hansen, F.D., and Carter, N.L. (1982) Creep of selected crustal rocks at 1000 MPa. *Eos Transactions American Geophysical Union*, 63, 437.
- Jackson, J.A. (2002) Strength of the continental lithosphere: Time to abandon the jelly sandwich ? *GSA Today*, 12, 9, 4-10.
- Jordan Seismological Observatory (JSO) (1993) Earthquakes in Jordan and Adjacent Areas, 25, Amman, Jordan, 1-142.
- Kirby, S.H. (1983) Rheology of the lithosphere. *Reviews of Geophysics and Space Physics*, 21, 6, 1458-1487.
- Kameyama, M., Yuen, D.A., and Karato, S.-I. (1999) Thermal-mechanical effects of low-temperature plasticity (the Peierls mechanism) on the deformation of a viscoelastic shear zone. *Earth and Planetary Science Letters*, 168, 159-172.
- Kissling, E. (1988) Geotomography with local earthquake data. *Review of Geophysics*, 26, 4, 659-698.
- Kissling, E., Ellsworth, W.L., Eberhart-Phillips, D., and Kradolfer, U. (1994) Initial reference models in local earthquake tomography. *Journal of Geophysical Research*, 99, 19635-19646.
- Mackwell, S.J, Zimmerman, M.E., and Kohlstedt, D.L. (1998) High-temperature deformation of dry diabase with applications to tectonics on Venus. *Journal of Geophysical Research*, 103, B1, 975-984.
- Maggi, A., Jackson, J.A., McKenzie, D., and Priestley, K. (2000) Earthquake focal depths, effective elastic thickness, and the strength of the continental lithosphere. *Geology*, 28, 6, 495-498.
- McKenzie, D., and Fairhead, D. (1997) Estimates of the effective elastic thickness of the continental lithosphere from Bouguer and free air gravity anomalies, *Journal of Geophysical Research*, 102, 27523-27552.
- Meissner, R., and Strehlau, L. (1982) Limits of stresses in continental crusts and their relation to the depth-frequency distribution of shallow earthquakes. *Tectonics*, 1, 73-89.
- Neev, D., and Hall, J. (1979) Geophysical investigations in the Dead Sea. *Sedimentary Geology*, 23, 209-238.

- Nyblade, A.A., and Langston, C.A. (1995) East African earthquakes below 20 km and their implications for crustal structure. *Geophysical Journal International*, 121, 49-62.
- Pe'eri, S., Wdowinski, S., Shtibelman, A., Bechor, N., Bock, Y., Nikolaidis, R., and van Domselaar, M. (2002) Current plate motion across the Dead Sea Fault from three years of continuous GPS monitoring. *Geophysical Research Letters*, 10.1029/2001GL013879.
- Prodehl, C., Fuchs, K., and Mechie, J. (1997) Seismic-refraction studies of the Afro-Arabian rift system – a brief review. *Tectonophysics*, 278, 1-13.
- Quennell, A.M. (1958) The structural and geomorphic evolution of the Dead Sea rift. *Quarterly Journal of the Geological Society of London*, 114, 1-24.
- Ranalli, G. (1987) *Rheology of the Earth: Deformation and flow processes in geophysics and geodynamics*. Allen and Unwin, Boston, MA.
- Ranalli, G., and Murphy, D.C. (1987) Rheological stratification of the lithosphere. *Tectonophysics*, 132, 281-295.
- Rodgers, J.J.W., and Adams, J.A.S. (1969) Uranium and Thorium. In Wedepohl, K.H. (Ed.) *Handbook of Geochemistry*, Vol. II/1: Springer, Berlin, 92K1-92K8 and 90K1-90K3.
- Rybach, L., and Buntebarth, G. (1984) The variation of heat generation, density and seismic velocity with rock type in the continental lithosphere. *Tectonophysics*, 103, 335-344.
- Scholz, C.H. (2002) *The Mechanics of Earthquakes and Faulting*, 2nd edition. Cambridge University Press, Cambridge, England.
- Shapira, A. (1997) On the seismicity of the Dead Sea basin. In Niemi, T.M., Ben -Avraham, Z., and Gat, J.R. (Eds.) *The Dead Sea: The lake and its settings*: Oxford University Press, New York, NY, 36, 82-86.
- Shapira, A., Avni, R., and Nur, A. (1993) A note: New estimate of the Jericho earthquake epicenter of July 11, 1927. *Israel Journal of Earth Sciences*, 42, 93-96.
- Shelton, G., and Tullis, J.A. (1981) Experimental flow laws for crustal rocks (abstract). *Eos Transactions American Geophysical Union*, 62, 396.
- Shudofsky, G., Cloetingh, S., Stein, S., and Wortel, R. (1987) Unusually deep earthquakes in East Africa: Constraints on the thermo-mechanical structure of a continental rift system. *Geophysical Research Letters*, 14, 741-744.
- Sibson, R.H. (1974) Frictional constraints on thrust, wrench and normal faults. *Nature*, 249, 542-544.
- Stiller, M., Yanaki, N.E., and Kronfeld, J. (1985) Comparative isotope study of two short sediment cores from the Dead Sea. *Chemical Geology (Isotope Geoscience Section)*, 58, 107-119.

- ten Brink, U.S. (2002) Corrigendum to 'Lower crustal flow and the role of shear in basin subsidence: an example from the Dead Sea basin'. *Earth and Planetary Science Letters*, 201, 447-448.
- ten Brink, U.S., and Ben-Avraham, Z. (1989) The anatomy of a pull-apart basin: seismic reflection observations of the Dead Sea basin. *Tectonics*, 2, 333-350.
- ten Brink, U.S., Kovach, R.L., Schoenberg, N., and Ben-Avraham, Z. (1990) Uplift and a possible Moho offset across the Dead Sea transform. *Tectonophysics*, 180, 71-85.
- ten Brink, U.S., Ben-Avraham, Z., Bell, R., Hassouneh, M., Coleman, D., Andreasen, G., Tibor, G., and Coakley, B. (1993) Structure of the Dead Sea pull-apart basin from gravity analysis. *Journal of Geophysical Research*, 98, 21877-21894.
- Thurber, C.H. (1984) SIMUL3. In Engdahl, E.R. (Ed.) *Documentation of Earthquake Algorithms: Report SE-35*, World Data Center A for Solid Earth Geophysics, Boulder, Colorado, 15-17.
- Turcotte, D.L., and Schubert, G. (2002) *Geodynamics*, 2nd edition. Cambridge University Press, Cambridge, England.
- Turcotte, T., and Arieh, E. (1988) Catalog of earthquakes in and around Israel. In *Preliminary safety analysis report: Israel Electric Corporation*, Tel Aviv, 1-18.
- van Eck, T., and Hofstetter, A. (1989) Microearthquake activity in the Dead Sea region. *Geophysical Journal International*, 99, 605-620.
- van Eck, T., and Hofstetter, A. (1990) Fault geometry and spatial clustering of microearthquakes along the Dead Sea-Jordan rift fault zone. *Tectonophysics*, 180, 15-27.
- Wong, I., and Chapman, D. (1990) Deep intraplate earthquakes in the western United States and their relationship to lithospheric temperatures. *Bulletin of the Seismological Society of America*, 80, 589-599.